УДК 550.385 DOI: https://doi.org/10.24028/gj.v47i2.322473

Magnitude of the anomalous geomagnetic fields

I.I. Rokityansky, A.V. Tereshyn, 2025

S. Subbotin Institute of Geophysics of National Academy of Sciences of Ukraine, Kyiv, Ukraine

The normalized amplitudes of the anomalous geomagnetic field variations (presented by tipper **C**) with period T>200 s arising around electrical conductivity anomalies have been considered. **C**>1 means that the secondary (induced) field is greater than the primary (inducing) one. Worldwide, the mean observed tippers are **C**=0.3 for coastal observatories and **C**=0.15 for inland ones. The maximum tippers are 1.5 for coastal and **C**=1.6 for inland observatories. Modeling realistic anomalies with uniform conductivity yields **C** up to 2.5. The larger **C** can arise in a non-uniform conductor due to the superchanneling effect.

Key words: electrical conductivity anomaly, normalized anomalous field, inductive anomaly, conductive anomaly, superchanneling.

Citation: Rokityansky, I.I., & Tereshyn, A.V. (2025). Magnitude of the anomalous geomagnetic fields. *Geofizychnyi Zhurnal*, *47*(2), 136—141. https://doi.org/10.24028/gj.v47i2.322473.

Introduction. Alternating EM fields used in deep geoelectrics and observed at the Earth's surface are induced by the currents in the ionosphere and magnetosphere. The lower atmosphere is assumed to be non-conductive. Therefore, the induced fields have a transverse-electric structure, i.e., electric fields and currents do not have a vertical component inside the horizontally-layered Earth.

Observations reveal anomalous behavior of geomagnetic variations in some areas. It can be explained only by electrical conductivity anomalies. In the middle of the 20th century, such anomalies were discovered in different parts of the world. Their normalized amplitudes were not expected to exceed 1 because the secondary (induced) field cannot be greater than the primary (inducing) one. This conclusion would be correct if the rocks enclosing an anomalous conductor were insulators, as was believed at that time. However, during the International Geophysical Year, a normalized anomalous horizontal field b_x greater than 2 and a vertical field b_z of magnitude 1.5 were measured at the Alert observatory and around it. Dyke and Garland (see reference in [Praus et al., 1971]) performed physical modeling, which showed that the main effect in the observed field was due to conductive redistribution of the regional currents in the enclosing medium rather than local electromagnetic induction.

Theory. Rokityansky [1982] showed that the conductive-type anomalous fields almost always prevail over the fields of local induction. A quantitative theory was created to describe it. The theory is based on an analytical solution for a cylinder presented as an infinite series with the first term proportional to the applied electric field E_0 (it forms a conductive-type anomaly) and the second one proportional to the magnetic field B_0 (it describes an inductive-type anomaly). Let us write them in a rectangular coordinate system with the center on the cylinder axis (Fig. 1).

$$\begin{Bmatrix} B_{xa} \\ B_{ya} \\ B_{za} \end{Bmatrix} = -\mu E_0 \sigma_i V\left(k_i a, \frac{\sigma_i}{\sigma_e}\right)\frac{a^2}{2r}\begin{Bmatrix} \cos\varphi \\ 0 \\ \sin\varphi \end{Bmatrix} - B_0 D\left(k_i a\right)\frac{a^2}{r^2}\begin{Bmatrix} \cos\varphi \\ 0 \\ \sin\varphi \end{Bmatrix}. \quad (1)$$

Since the cylinder is a 2D anomaly, and we study the anomalous fields in the geomagnetic components, let us consider only the E-polarization case. The electric field E_0 is formed by the large-scale regional external sources directed along the anomalous cylinder y axis. The primary normal magnetic field B_0 is formed by external and internal (induced in a horizontally layered Earth) currents along the x axis.

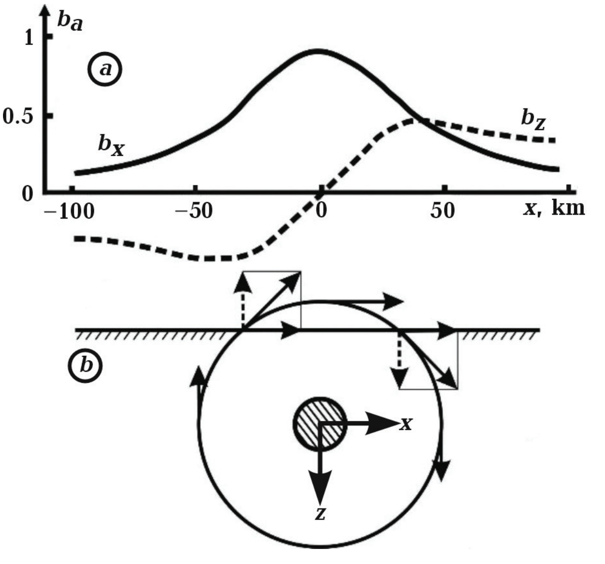

Fig. 1. Formation of the anomalous fields around a circular cylinder: a — profile graphs, b — anomalous field decomposition into b_x and b_z components.

In Eq. 1, a is the cylinder's radius, σ_i and σ_e — electrical conductivity of the cylinder and the enclosing medium, $k_i=(i\omega\mu\sigma_i)^{1/2}$, μ — magnetic permeability, $\omega=2\pi/T$, T — period, $r=(x^2+z^2)^{1/2}$ — the distance at which the anomalous field B_a is studied. The angle φ is measured from the direction of the vertical axis z. D is the decreasing (from 1 to 0) function of the period.

Normalizing the anomalous fields to the normal field B_{0x}, we obtain non-dimensional anomalous fields b_x and b_z, which we present only for the conductive-type anomaly in the form

$$\begin{Bmatrix} b_x \\ b_z \end{Bmatrix} = A(r)V(T)\zeta(T)\begin{Bmatrix} \cos\varphi \\ \sin\varphi \end{Bmatrix}, \qquad (2)$$

$A=\mu\sigma_i a^2/2r$ depends on geometric factors.

V is an increasing function of the period describing the degree of filling of the conductor with the anomalous currents. At $T\to0$, the skin-effect does not allow the current to penetrate the conductor and $V\to0$. At $T\to\infty$ the anomalous currents fill the entire conductor and $V\to1-\rho_i/\rho_e$.

$\zeta=E_{0y}/B_{0x}$ is the impedance of 1D (horizontally or spherically) layered enclosing medium. It is a decreasing function of the period.

The product of the increasing and decreasing functions has a maximum at some period T_0. T_0 depends on the parameters of the anomaly (V) and the enclosing medium (ζ).

Numerous calculations for the deep crustal conductors and the seawater of different depth and configurations show (Fig. 2) that the T_0 position is closely related to the total lengthwise conductance of the anomaly G[S·m]$=Q\cdot s_i$ (Q is the cross-section area) by the equation $G[\text{S·m}]=5\cdot10^4\,|\,T_0[\text{s}]\,|^{\,1.2}$. This dependence is also presented in Fig. 3. The upper red line is obtained from calculations of the deep crustal models. The lower blue line is obtained from the sea models using only the tipper data. The difference between the two lines does not exceed the uncertainties of their determination.

Results of measurements. We processed the geomagnetic field recorded in 137 worldwide distributed observatories of the INTERMAGNET network (https://www.intermagnet.org) and 14 Japanese ones from 1991 to 2014. We obtained the induction arrows for the periods 150—3600 s (Fig. 4).

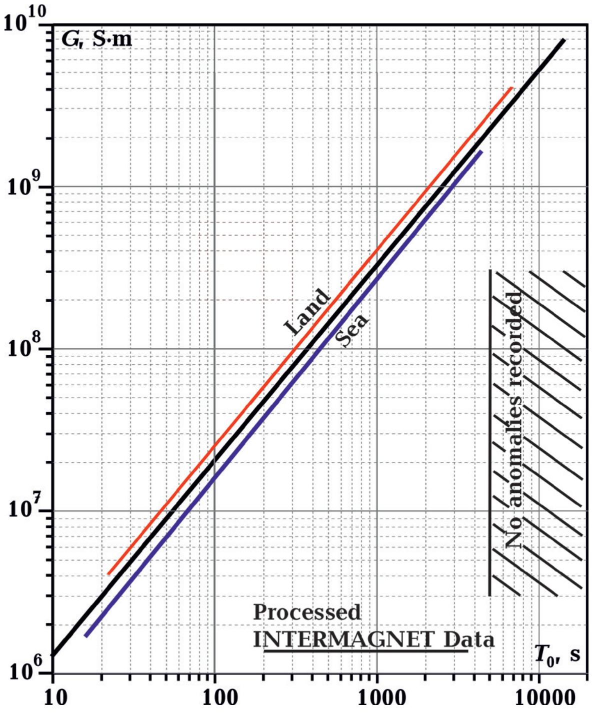

Fig. 3. The relationship between conductance G and period T_0 at which the anomalous field reaches maximum.

The distribution of the induction arrows' magnitude differ for the coastal and inland observatories. So, the median magnitude is 0.3 for the coastal observatories and 0.15 for inland ones. The largest magnitudes are observed at the coastal observatories opposite deep seawater: DRV (Antarctica) **C**=1.5, STJ, (Newfoundland) **C**=1.3, ALB (SW Australia) **C**=1.3, NAQ (S Greenland) **C**=1, HER (S Africa) **C**=1, and KOU (NE South America) **C**=0.9. At all the rest of the INTERMAGNET observatories, the magnitude was less than 0.8. However, inland, many short-term field observations are performed, and some have found strong anomalies. The largest induction arrow **C**=1.6 was registered at site PYAT [Rokityansky, Tereshyn, 2022] on the Donbas anomaly in eastern Ukraine. A slightly less **C**=1.5 was found at Cape Mary Cleverly [Praus et al., 1971] on the Alert anomaly in northeast Canada.

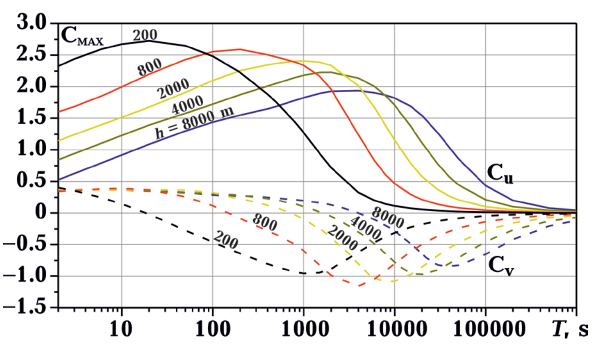

Fig. 2. Induction arrows frequency characteristics on the coast of the h m deep rectangular sea.

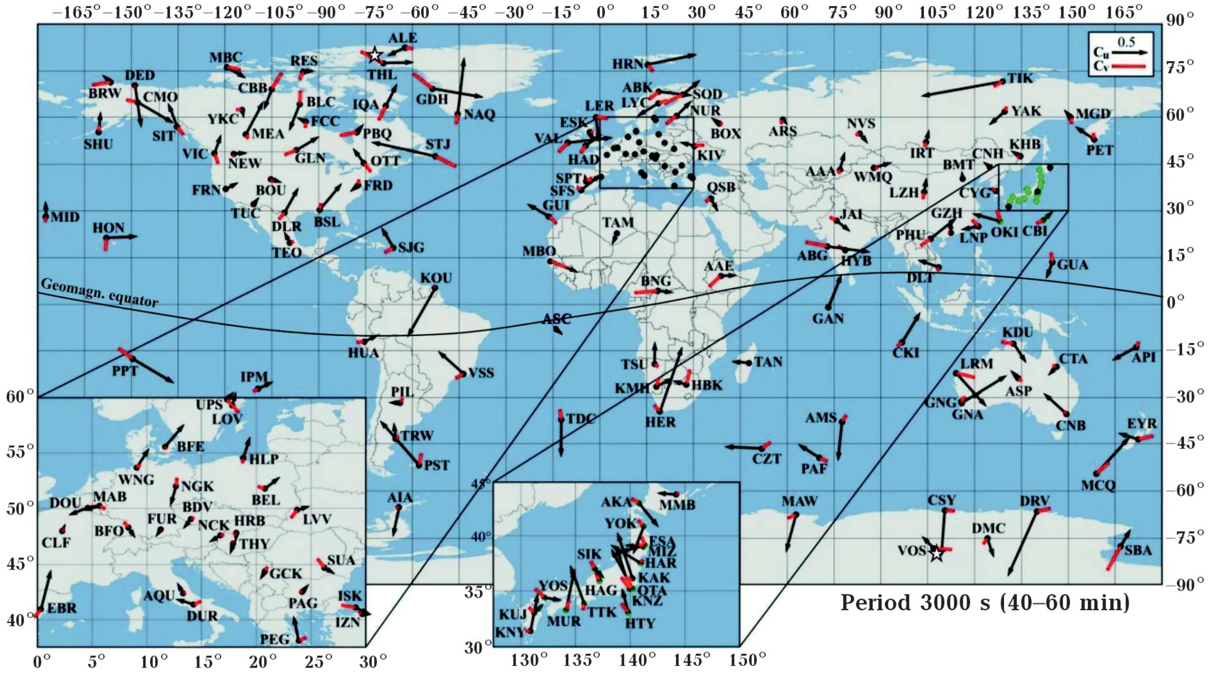

Fig. 4. The real $\mathbf{C}_u$ and imaginary $\mathbf{C}_v$ induction arrows for the period 3000 s (40—60 min) in 137 INTERMAGNET and 14 Japanese observatories. Geomagnetic poles for 2010 are marked by the 5-ray stars.

A sensational article in the EPS journal [Xu et al., 2023] reported induction arrows with magnitude $\mathbf{C}>3$ in 3 sites in SW China. The authors' 3D model yields $\mathbf{C}>3$. They concluded that their modeling supports high magnitudes obtained in the field.

Discussion. We checked the model in [Xu et al., 2023], and it turned out that instead of the real upper mantle with rapidly increasing electrical conductivity, a half-space with a high resistance of 10,000 Ohm·m was used. This is strange because among the authors of the work [Xu et al., 2023] was Kuvshinov, who carried out the most accurate determinations of the electrical conductivity growth in the upper mantle. We performed the same modeling with half-space and real well-conducting mantle based on [Kuvshinov et al., 2021] and obtained $\mathbf{C}$=3.2 and 1.2 respectively. Only the second result corresponds to the real Earth. We thought about how to explain such large anomalous fields and concluded that they could arise in an elongated conductor with a non-uniform cross-section Q along its strike.

These calculations and recommendations for the authors to check the measurements were compiled as comments and sent to the EPS Editor. Reviewers approved them but recommended making some clarifications and improving the English language. We did all this and waited two months for the comment to be published. However, we received another review with quite new critical requirements. We understood that our comments would be rejected. In January 2025, our colleague who worked in China informed us that «enormously large tippers» were obtained by mistake; in fact, they are significantly lower, and the EPS has been waiting for months for an explanation from the Chinese authors. We understood why our comments were rejected.

Wider discussion. Frequency characteristics of the tipper from conductors with different cross-section areas are presented in Fig. 2. With increasing sea depth, G and T_0 also increase. However, why does the tipper's magnitude at T_0 and shorter periods becomes smaller the larger the conductor and its T_0? This occurs because, at longer periods, the influence of the deep conductivity of the mantle becomes stronger.

Our processing yields anomalous fields

in a narrow range of periods (150—3600 s). As shown in Fig. 2, frequency characteristics occupy more than three orders in the period scale. Therefore, our observations at 3000 s definitely must be sensitive to the anomalies with T_0 up to 30,000 s. However, neither our INTERMAGNET processing results nor any others measurements on long periods detected any anomaly with a period T_0 greater than 5000 s. According to Fig. 3, it means that anomalies with a lengthwise conductance $G>2\cdot10^9$ S·m are not found. It is an important geophysical result. It is shown on the right side of Fig. 3.

Are there any structures of electrical conductivity in/near which the tipper will exceed 3, given the Earth's well-conducting upper mantle? We calculated and analyzed many 2D models. Fig. 2 presents the largest tippers for maximum $\mathbf{C}_u$ (at a distance ≈h from the coast) obtained for an idealized sea cross-section with a *rectangular* shape. These modeled maximum magnitudes **C** are 2—2.5 for the studied periods T>200 s, which are 1.5-fold larger than the maximum observed **C** (1.5—1.6).

So, **C** cannot exceed 2—2.5 in the anomalous bodies with uniform conductivity and 2D or, especially, limited length structure. However, this is possible in a long conductor with a varying cross-section area Q in the places where Q is minimal. In these places the 3D phenomenon of superchanneling occurs. It was considered qualitatively in [Rokityansky 1982, p. 224—229]. A special 3D modeling investigation should be done for a quantitative description of superchanneling effect. To our knowledge, such an investigation has not been described anywhere (although many thousands of 3D-models have been made for specific structures interpretation, only a few computations have been performed to study the regularities of the electromagnetic field) and represents a challenge for 3D modeling.

Conclusions. The frequency characteristic maximum T_0 of all known electrical conductivity anomalies is less than 5000 s, imposing a limit on its lengthwise conductance G.

The median tipper magnitude is **C**=0.3 for coastal observatories and **C**=0.15 for inland ones. The maximal is **C**=1.6 for inland and 1.5 for coastal observatories.

Model calculations over uniform conductivity anomalies yield **C** up to 2.5. The larger **C** can arise in a lengthwise non-uniform conductor due to the superchanneling effect.

References

Kuvshinov, A., Grayver, A., Töfner-Clausen, L., & Olsen, N. (2021). Probing 3-D electrical conductivity of the mantle using 6 years of Swarm, CryoSat-2 and observatory magnetic data and exploiting matrix Q-responses approach. *Earth, Planets and Space*, *73*(67) https://doi.org/10.1186/s40623-020-01341-9.

Praus, O., De Laurier, J.M., & Law, L.K. (1971). The extension of the Alert geomagnetic anomaly through Northern Ellesmere Island, Canada. *Canadian Journal of Earth Sciences*, *8*(50), 50—64. https://doi.org/10.1139/e71-003.

Rokityansky, I.I. (1982) *Geoelectromagnetic investigation of the Earth's crust and upper mantle*. Berlin-Heidelberg-New York: Springer Verlag, 381 p. https://doi.org/10.1007/978-3-642-61801-7.

Rokityansky, I.I., & Tereshyn, A.V. (2022). Donbas geoelectrical structure. *Geofizychnyi Zhurnal*, *44*(1), 158—172. https://doi.org/10.24028/gzh.v44i1.253717.

Xu, S., Chen, C., Kruglyakov, M., Kuvshinov, A., Rigaud, R., & Hu, X. (2023). Enormously large tippers observed in southwest China: can realistic 3-D EM modeling reproduce them? *Earth, Planets and Space*, *75*, 109. https://doi.org/10.1186/s40623-023-01863-y.

Величина аномальних геомагнітних полів

І.І. Рокитянський, А.В. Терешин, 2025

Інститут геофізики ім. С.І. Субботіна НАН України, Київ, Україна

Розглянуто нормалізовані амплітуди варіацій аномального геомагнітного поля (представлені типпером **C**) з періодом *T*>200 с, що виникають навколо аномалій електропровідності. **C**>1 означає, що вторинне (індуковане) поле перевищує первинне (індукуюче) поле. У всьому світі спостережувані середні значення типперів становлять: **C**=0,3 для прибережних обсерваторій і **C**=0,15 для континентальних. Максимальні значення: **C**=1,6 для континентальних і 1,5 для прибережних обсерваторій. Під час моделювання реалістичних аномалій із однорідною провідністю отримано значення **C** до 2,5. Більші значення **C** можуть виникати у випадку неоднорідного провідника через ефект суперканалювання.

Ключові слова: аномалія електропровідності, нормоване аномальне поле, індуктивна аномалія, кондуктивна аномалія, суперканалювання.